State-Dependent Changes in the Electrostatic Potential in the Pore of a GluR Channel

Alexander I. Sobolevsky, Maria V. Yelshansky, and Lonnie P. Wollmuth
Department of Neurobiology and Behavior, State University of New York at Stony Brook, Stony Brook, New York 11794-5230

ABSTRACT The M2 loop and the M3 segment are the major pore-lining domains in the GluR channel. These domains determine ion permeation and channel block processes and are extensively involved in gating. To study the distribution of the membrane electric potential across the GluR channel pore, we recorded from α-amino-3-hydroxy-5-methylisoxazole-4-proprionic acid receptors containing M2 and M3 cysteine substitutions in the GluR-A subunit and measured the voltage dependence of the modification rate of these substituted cysteines by methanethiosulfonate reagents either in the presence or absence of glutamate. In the presence of glutamate, the voltage dependence became gradually stronger for positions located deeper in the pore suggesting that the electrostatic potential drops fairly uniformly across the pore in the open state. In contrast, in the absence of glutamate, the voltage dependence was biphasic. The difference in the electrostatic potential in the presence and absence of glutamate had an apparent maximum in the middle of the extracellular vestibule. We suggest that these state-dependent changes in the membrane electric potential reflect a reorientation of the dipoles of the M2 loop α-helices toward and away from the center of the channel pore during gating.

INTRODUCTION

The distribution of the electrostatic potential across the pore of an ion channel is critical to ion permeation and channel block mechanisms (Hille, 2001). This potential depends on numerous channel properties including local factors such as the molecular identity of side chains and global factors like pore geometry. Because the structure of the pore undergoes significant transformations during channel opening/closure, the distribution of the electrostatic potential across the pore can be state dependent. In the acetylcholine receptor channel, for example, a local ~200-mV change in the electrostatic potential caused by a ring of glutamate residues in the open state is nearly absent in the closed state (Pascual and Karlin, 1998; Wilson et al., 2000). Similarly, in bacterial K^+ channels with the intracellular gate at the crossing point of the TM2 helices in the closed conformation (KcsA), the electrostatic potential changes fairly uniformly across the entire channel pore, whereas when it is in the open conformation (MthK), the potential becomes concentrated across the narrow region of the selectivity filter (Jiang et al., 2002).

Ionotropic glutamate receptors (GluRs) are ligand-gated ion channels that mediate information processing at the majority of excitatory synapses in the brain and participate in such physiological processes as learning and memory, development and maintenance of cellular connections, and pain perception (Dingledine et al., 1999). Dysfunctional GluRs have also been implicated in numerous neurodegenerative and psychiatric disorders (Doble, 1999). The GluR channel shares a common design with a K^+ channel, although it is inverted in the membrane (for recent reviews see Kuner et al., 2003; Wollmuth and Sobolevsky, 2004). The major pore-lining domains in GluR channels, the M2 loop and the M3 segment (Fig. 1), are structurally similar to the P loop and the inner helix (TM2 in KcsA or MthK) in K^+ channels (Kuner et al., 1996, 2001; Panchenko et al., 2001; Sobolevsky et al., 2003). Additionally, the GluR M3 segment, like the homologous TM2 domain in K^+ channels, is extensively involved in channel gating (Kohda et al., 2000; Jones et al., 2002; Sobolevsky et al., 2002, 2003).

To study the electrostatic potential in GluRs, we took advantage of substituted cysteines located at different levels in the α-amino-3-hydroxy-5-methylisoxazole-4-proprionic acid receptor (AMPAR) channel pore and measured the voltage dependence of the rate of their modification by externally applied methanethiosulfonate (MTS) reagents. The voltage dependence was distinctly state dependent. In the presence of glutamate, the voltage dependence became gradually stronger for positions located deeper in the pore suggesting that the electrostatic potential drops fairly uniformly across the pore in the open state. Surprisingly, we find that a much greater portion of the transmembrane electric field drops across the narrow region of the pore (intracellular vestibule) in the closed than in the open state. We suggest that this state-dependent change in the electrostatic potential arises from a differential distribution of charges within the pore during gating. Structurally, this state-dependent charge distribution may be due to a movement of the M2 α-helix dipoles during gating with the negative (C-terminal) poles of these dipoles pointed toward the center of the pore in the open state and away from it in the closed state.

Submitted July 11, 2004, and accepted for publication October 19, 2004.

Address reprint requests to Dr. Alexander I. Sobolevsky, Dept. of Biochemistry and Molecular Biophysics, Columbia University, Rm. 513, Black Bldg., 650 W. 168th St., New York, NY 10032. Tel.: 212-305-4062; Fax: 212-305-8174; E-mail: as2642@columbia.edu.

0006-3495/05/01/235/08 $2.00

doi: 10.1529/biophysj.104.049411

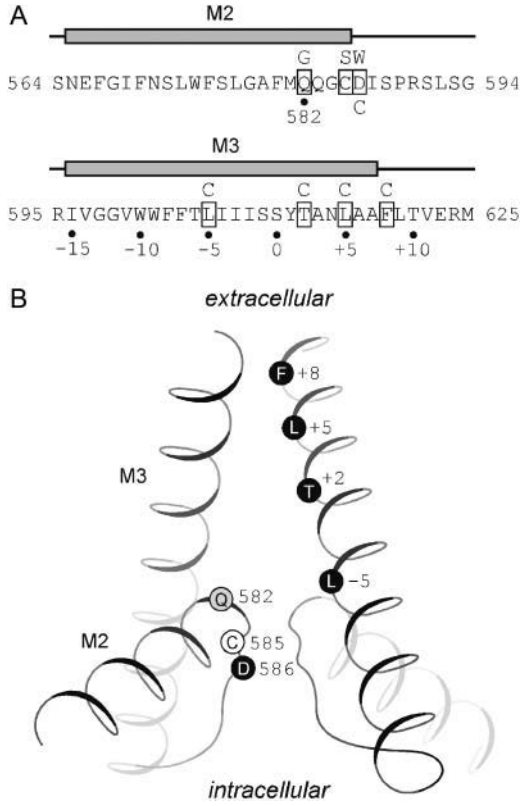

FIGURE 1 Presumed positioning of amino acid residues in the pore-lining domains M2 and M3 of AMPAR channels. (*A*) The amino acid sequence of the region encompassing the M2 loop and M3 segment in the AMPAR GluR-A subunit. Residues are shown in one-letter code. The numbering is for the mature protein. The amino acids in M3 are also numbered relative to the first position (S, position 611) in SYTANLAAF, the most highly conserved motif in GluRs. Shaded rectangles above the amino acid sequence outline the borders of M2 and M3. Open boxes highlight the positions where point mutations (specified above or below the sequence) were introduced. (*B*) Topology of the major pore-lining domains in AMPAR channels. The M2 loop and the M3 segment are shown for two of four GluR-A subunits with the back and front subunits removed. Presumed α-helical regions are shown as spirals. Native or substituted cysteines at highlighted positions are nonaccessible (*open circle*), accessible only in the presence of glutamate (*shaded circle*), or accessible both in the presence and absence of glutamate (*solid circles*) to extracellularly applied MTS reagents (Kuner et al., 2001; Sobolevsky et al., 2003). The Q/R site (Q582) is presumably located at the tip of the M2 loop.

METHODS

Mutagenesis and heterologous expression

All mutations were introduced into a GluR-A (flip form) expression construct where a leucine in the ligand-binding domain was substituted with a tyrosine (L479Y). GluR-A(L479Y) receptors, referred to here as wild type (wt′), are essentially nondesensitizing (Stern-Bach et al., 1998). Point mutations (see Table 1 for a detailed description) were generated as described (Sobolevsky et al., 2003). cRNA was transcribed and capped for each expression construct using SP6 RNA polymerase (Ambion, Austin, TX) and examined electrophoretically on a denaturating agarose gel. RNA concentrations were determined by ethidium bromide stain of the gel relative to an RNA molecular weight marker. Dilutions of RNA (0.01–0.1 μg/μl) were prepared to achieve optimal expression. Nondesensitizing wt′ or mutant subunits were expressed in *Xenopus laevis* oocytes. Oocytes were prepared, injected, and maintained as described (Wollmuth et al., 1996; Sobolevsky et al., 2002). Recordings were made 1–6 days after injections.

Recording conditions and solutions

Whole-cell currents of *Xenopus* oocytes were recorded at room temperature (20–23°C) using two-electrode voltage clamp (DAGAN TEV-200A, DAGAN, Minneapolis, MN) with Cell Works software (npi electronic GmbH, Tamm, Germany). Microelectrodes were filled with 3 M KCl, and had resistances of 1–4 MΩ. To minimize solution exchange rates, we used a narrow flow-through recording chamber with a small volume of ~70 μl. The external solution consisted of (mM): 115 NaCl, 2.5 KCl, 0.18 $CaCl_2$, and 10 HEPES (pH 7.2, NaOH). Glutamate (1 mM), CNQX, and MTS reagents were applied with the bath solution.

AMPAR cysteine-substituted mutant channels were probed from the extracellular side of the membrane with MTS reagents, 2-aminoethyl MTS (MTSEA), 2-(trimethylammonium)ethyl MTS (MTSET), and methyl MTS (MMTS). MTS reagents were purchased from Toronto Research Chemicals (Ontario, Canada) and were prepared, stored, and applied as described (Sobolevsky et al., 2002). All other chemicals were obtained from Sigma (St. Louis, MO). Reaction rates in the presence, $k_{+\mathrm{Glu}}$, or absence, $k_{-\mathrm{Glu}}$, of glutamate were determined using ''pulsive'' protocols (see Fig. 2) as described in detail in (Sobolevsky et al., 2002).

Data analysis

Data analysis was done using Igor Pro (WaveMetrics, Lake Oswego, OR) and Microcal Origin 4.1 (Northampton, MA). For analysis and display, leak currents were subtracted from total currents. Results are presented as mean ± SE. An analysis of variation or a Student's *t*-test was used to test for statistical differences. The Tukey test was used for multiple comparisons. Significance was assumed if $P < 0.05$.

The voltage dependence of the apparent second-order rate constants for MTS modification measured in the presence, $k_{+\mathrm{Glu}}$, or absence, $k_{-\mathrm{Glu}}$, of glutamate was analyzed according to the following equations:

$$k_{+\mathrm{Glu}} = k^0_{+\mathrm{Glu}} \exp(-z\delta_{+\mathrm{Glu}} FV_h/RT), \quad (1)$$

$$k_{-\mathrm{Glu}} = k^0_{-\mathrm{Glu}} \exp(-z\delta_{-\mathrm{Glu}} FV_h/RT), \quad (2)$$

where V_h is the holding membrane potential, $k^0_{+\mathrm{Glu}}$ and $k^0_{-\mathrm{Glu}}$ are the values of $k_{+\mathrm{Glu}}$ and $k_{-\mathrm{Glu}}$ at $V_h = 0$, $\delta_{+\mathrm{Glu}}$ and $\delta_{-\mathrm{Glu}}$ are the presumed fractions of the transmembrane electric field the MTS reagent passes to reach the exposed cysteine, and z is the charge of the reagent. F, R, and T have their usual meaning. To derive $z\delta_{+\mathrm{Glu}}$ and $z\delta_{-\mathrm{Glu}}$, we rearranged Eqs. 1 and 2:

$$-(RT/F)\mathrm{Ln}\, k_{+\mathrm{Glu}} = A_{+\mathrm{Glu}} + z\delta_{+\mathrm{Glu}} V_h, \quad (3)$$

$$-(RT/F)\mathrm{Ln}\, k_{-\mathrm{Glu}} = A_{-\mathrm{Glu}} + z\delta_{-\mathrm{Glu}} V_h, \quad (4)$$

where $A_{+\mathrm{Glu}}$ and $A_{-\mathrm{Glu}}$ are $-(RT/F)$ Ln $k^0_{+\mathrm{Glu}}$ and $-(RT/F)$ Ln $k^0_{-\mathrm{Glu}}$, respectively, and fitted Eqs. 3 and 4 to plots of $-(RT/F)$ Ln $k_{+\mathrm{Glu}}$ or $-(RT/F)$ Ln $k_{-\mathrm{Glu}}$ against V_h.

The voltage dependence of AMPAR channel block by polyamines was estimated by the method described previously (Panchenko et al., 1999, 2001). Briefly, membrane currents generated using voltage ramps (0.1 Vs^{-1}) were recorded either in the absence or presence of glutamate. These current-voltage (*I-V*) dependencies were subtracted and fitted with a 15-order polynomial function to estimate the reversal potential, V_{rev}. Conductance-voltage (*G-V*) plots were then generated and fitted with the following Boltzmann function over the range from −100 to +20 mV:

$$G = G_{max}/(1 + \exp((V - V_b)/k_b)), \quad (5)$$

where V is the membrane potential, G_{max} is the conductance at a sufficiently hyperpolarized potential to produce full relief from block by polyamines, V_b is the potential at which 50% block occurs, and k_b is a slope factor describing the voltage dependence of block.

RESULTS

To characterize the electrostatic potential across the pore of the AMPAR channel, we measured the voltage dependence of the rate of reactivity of MTS reagents with substituted cysteines. We focused on cysteines introduced at five positions in the pore-forming M2 and M3 domains that are accessible to extracellularly applied MTS reagents both in the presence (closed and open states) and absence (closed state) of glutamate (Kuner et al., 2001; Sobolevsky et al., 2003). Four of these positions are located in the M3 segment (L−5, T+2, L+5, and F+8) and one (D586) is in the M2 loop (Fig. 1). Labels and a description of mutant GluR-A subunits containing cysteine substitutions at these five positions are listed in Table 1. Initially, we measured modification rates of cysteine-substituted AMPAR channels by MTS reagents in the presence or absence of glutamate.

State-dependent modification rates of cysteine-substituted AMPAR channels

Fig. 2, *A* and *B*, illustrate our protocols to measure modification rates in the presence or absence of glutamate. The MTS reagent (*open box*; 1 min) was applied five times either in the presence of glutamate (*thin lines*) (Fig. 2 *A*) or in the absence of glutamate but in the presence of the competitive AMPAR antagonist CNQX (10 μM; *shaded boxes*) (Fig. 2 *B*). Glutamate-activated current amplitudes were fitted with a single exponent as a function of the cumulative time of the MTS reagent exposure. The time constants of these fits, τ_{+Glu} or τ_{-Glu}, defined the apparent second-order rate constants for chemical modification in the presence, $k_{+Glu} = 1/(\tau_{+Glu} \times [MTS])$, or absence, $k_{-Glu} = 1/(\tau_{-Glu} \times [MTS])$, of glutamate, where $[MTS]$ is the concentration of the MTS reagent.

The values of k_{+Glu} and k_{-Glu} measured for MTSEA at the holding potential (V_h) of −60 mV are summarized in Table 1. For positions deeper than L+5C, modification rates in the presence of glutamate were always faster than those in the absence of glutamate. This result is consistent with previous ones (Sobolevsky et al., 2002, 2003) and supports the idea that the extracellular vestibule of GluR channel in the closed state is narrower than in the open state.

Modification rates of substituted cysteines depend on a number of factors (Karlin and Akabas, 1998) including (among others): the acid dissociation of the cysteine thiol group; the local and global steric constraints such as the size of the water-filled pathway leading up to the substituted cysteine; and for charged reagents, the electrostatic potential along the pathway and at the residue. This latter feature permits the use of charged MTS reagents to probe the electrostatic potential at the substituted cysteine by measuring the modification rate at different membrane voltages (Pascual and Karlin, 1998; Wilson et al., 2000).

Voltage dependence of modification rates

To characterize the electrostatic potential at the substituted cysteine in AMPAR channel, we measured modification rates as illustrated in Fig. 2, *A–B*, at different holding potentials. Fig. 2 *C* shows the modification rate constants for Q582G/T+2C channels measured at different V_h both in

TABLE 1 Modification rate constants and polyamine block in mutant AMPAR channels

Mutant		Modification rate constants at −60 mV		Polyamine block	
Label	Description	k_{+Glu} $M^{-1}s^{-1}$	k_{-Glu} $M^{-1}s^{-1}$	V_b mV	k_b mV
wt′	GluR-A(L479Y)	ND	ND	−41.8 ± 4.6	13.8 ± 0.5
F+8C	GluR-A(L479Y/F619C)	4710 ± 256	2528 ± 112	−60.8 ± 4.4	15.5 ± 0.4
L+5C	GluR-A(L479Y/L616C)	42.1 ± 1.3	77.8 ± 2.0	−74.5 ± 2.1	20.3 ± 0.5
T+2C	GluR-A(L479Y/T613C)	6406 ± 255	87.4 ± 8.2	−42.8 ± 2.1	14.3 ± 0.4
Q582G/T+2C	GluR-A(L479Y/Q582G/C585S/T613C)	819 ± 29	247 ± 10	−3.2 ± 3.0	20.2 ± 1.2
D586W/T+2C	GluR-A(L479Y/C585S/D586W/T613C)	609 ± 30	151 ± 15	ND	ND
L−5C	GluR-A(L479Y/L606C)	314 ± 8	15.6 ± 1.2	−40.3 ± 7.1	14.0 ± 0.7
D586C	GluR-A(L479Y/C585S/D586C)	4839 ± 165	12.7 ± 0.3	ND	ND

Values shown are means ± SE. Modification rate constants (k_{+Glu} and k_{-Glu}) are for MTSEA (n = 4–6). Parameters for polyamine block (V_b and k_b) were estimated using Eq. 5 fitted to G-V plots (n = 5–11) (see Methods for details). ND, not defined.

Description of mutants. The L479Y mutation was introduced into the wild-type GluR-A subunit, referred to here as wt′, to create a nondesensitizing AMPAR (Stern-Bach et al., 1998). This nondesensitizing construct was used as a background for all additional mutations used in this study. Cysteine substitutions (M2 loop, D586C; M3 segment, L606C, T613C, L616C, and F619C) were introduced at five positions accessible both in the presence and absence of glutamate to extracellularly applied MTS reagents (Kuner et al., 2001; Sobolevsky et al., 2003) (Fig. 1). Two residues in M2 (Q582 and D586) were substituted with glycine (Q582G) or tryptophan (D586W) to disrupt polyamine block (Panchenko et al., 1999). To avoid possible mutation-induced accessibility of the native cysteine C585, substitutions in M2 were introduced in the C585S background. When mutations were introduced only in M3, C585 was considered nonaccessible (Sobolevsky et al., 2003).

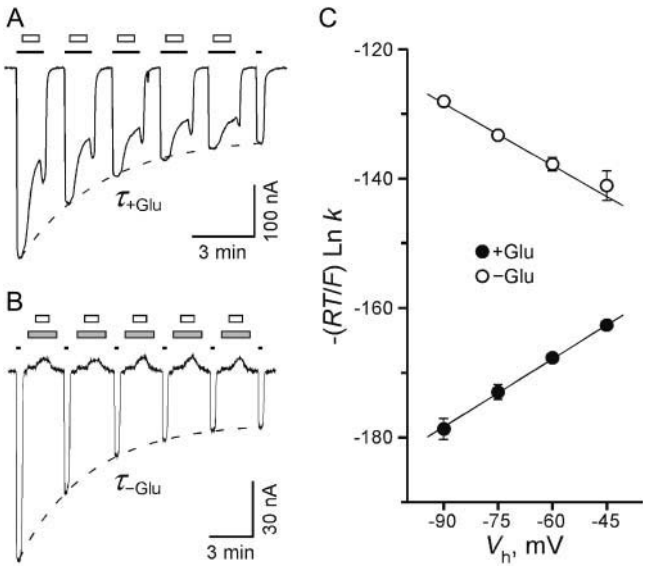

FIGURE 2 Voltage-dependent kinetics of substituted cysteine modification by MTS reagents. (*A*, *B*) Pulsive protocols to assay modification rates of exposed cysteines in the presence (*A*) (+Glu) or absence (*B*) (−Glu) of glutamate. The examples show Q582G/T+2C channels (see description in Table 1). The membrane potential, V_h, was −60 mV. (*A*) The MTSEA application (10 μM; *open box*; 1 min) was started 15 s after the beginning and finished 15 s before the end of the glutamate (*thin line*) application. The cell was washed for 1.5 min between glutamate applications. Current amplitudes, defining the time course of cysteine modification, were measured during the first 15 s of each glutamate exposure and fitted with a single exponent as a function of cumulative MTSEA exposure (*dashed line*; $\tau_{+Glu} = 103 \pm 4$ s). (*B*) One minute after the 15-s test glutamate application (*thin line*), CNQX (10 μM; *shaded box*) was applied for 1.5 min. The MTSEA application (50 μM; *open box*; 1 min) was started 15 s after the beginning and finished 15 s before the end of the CNQX exposure. After CNQX, the cell was washed for 1.25 min before the next test glutamate application. Similar to panel *A*, current amplitudes were fitted with a single exponential function (*dashed line*; $\tau_{-Glu} = 88 \pm 3$ s). (*C*) Voltage dependence of modification rates. Apparent second-order rate constant for MTSEA modification of Q582G/T+2C channels, expressed in a logarithmic form (−(*RT*/*F*)*Ln*k*), as a function of V_h. The rate constants for modification in the presence (*solid circles*) and absence (*open circles*) of glutamate were estimated using the protocols illustrated in panels *A* and *B*, respectively. Some error bars are smaller than the symbol size. The straight lines through the points are fits with Eqs. 3 ($z\delta_{+Glu} = 0.35 \pm 0.01$) and 4 ($z\delta_{-Glu} = -0.32 \pm 0.02$).

the presence (*solid circles*) or absence (*open circles*) of glutamate. Consistent with previous results (Sobolevsky et al., 2003), membrane hyperpolarization increased the modification rate of T+2 cysteine in the presence of glutamate. Surprisingly, in the absence of glutamate, membrane hyperpolarization caused the modification rate of T+2C to decrease. The slope of the fitted line to plots such as those illustrated in Fig. 2 *C* yields an estimate of the apparent fraction of the membrane electric field the MTS reagent passes to reach the exposed cysteine (δ) multiplied by the reagent's charge (z) (see Methods). For Q582G/T+2C channels, the $z\delta$ value measured in the presence of glutamate ($z\delta_{+Glu}$) was ~0.35, whereas in the absence of glutamate ($z\delta_{-Glu}$) it was ~−0.32.

Fig. 3 summarizes the $z\delta_{+Glu}$ and $z\delta_{-Glu}$ values measured for the different mutant channels. In all instances, $z\delta_{+Glu}$ values were positive (*top*). They also became gradually greater for positions in M3 located deeper in the pore (cf. Figs. 1 *B* and 3) with the highest value (0.73 ± 0.02) measured for L−5, which is presumably located just external to the tip of the M2 loop. In contrast, the voltage dependence of reactivity was relatively weak ($z\delta_{+Glu} = 0.25 \pm 0.01$) for a cysteine substituted in M2 (D586), which is presumably located deeper in the pore than L−5 (see Fig. 1 *B*). The negative charge of the aspartate side chain at 586 may therefore contribute to the electrostatic potential. On the other hand, substitution of D586 with tryptophan in D586W/T+2C channels resulted only in a slight reduction of $z\delta_{+Glu}$ for cysteine substituted at T+2 (cf., $z\delta_{+Glu} = 0.25 \pm 0.01$ for D586W/T+2C and $z\delta_{+Glu} = 0.30 \pm 0.02$ for T+2C). Together, the data for D586C, D586W/T+2C, and T+2C channels suggest that the effect of D586 charge neutralization on the membrane electric potential sensed by MTS

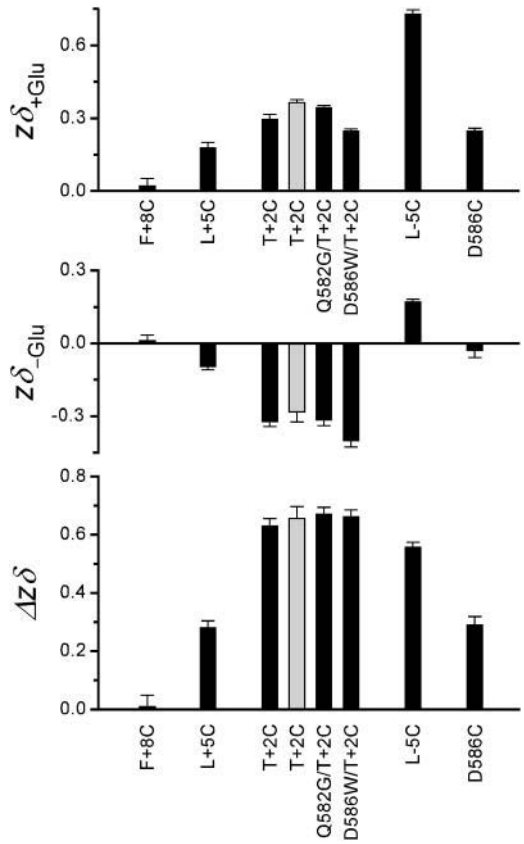

FIGURE 3 State-dependent changes in the membrane electric potential sensed by MTS reagents. The mean values of $z\delta_{+Glu}$ (*top*) and $z\delta_{-Glu}$ (*middle*) estimated using the approach illustrated in Fig. 2 and their difference $\Delta z\delta$ (*bottom*). Solid and shaded bars show the data for MTSEA and MTSET, respectively. The $z\delta_{+Glu}$ values for L−5C, T+2C (MTSEA), L+5C, and F+8C are taken from (Sobolevsky et al., 2003).

reagents is strong in close proximity to D586 but becomes much weaker for distant positions, specifically those located in the extracellular vestibule.

In the absence of glutamate (Fig. 3, *middle*), the modification rate for the most external position tested, F+8C, was voltage independent ($z\delta_{-Glu} = 0.01 \pm 0.02$) like in the presence of glutamate ($z\delta_{+Glu} = 0.02 \pm 0.03$). For positions presumably located in the middle of the extracellular vestibule, $z\delta_{-Glu}$ was negative ($z\delta_{-Glu} = -0.10 \pm 0.01$ for L+5C and $z\delta_{-Glu} = -0.32 \pm 0.02$ for T+2C), becoming positive at the deepest position in M3, L−5C ($z\delta_{-Glu} = 0.18 \pm 0.01$). The negative values of $z\delta_{-Glu}$ for positions in the middle of the extracellular vestibule define the bell-shaped difference between $z\delta_{+Glu}$ and $z\delta_{-Glu}$ as a function of substituted cysteine location (Fig. 3, *bottom*) with the apparent maximum at T+2 ($\Delta z\delta = 0.63 \pm 0.02$).

Because under our experimental conditions, a small portion of MTSEA molecules is uncharged, this neutral form of MTSEA may cross the membrane and react with substituted cysteines from the cytoplasmic side (Holmgren et al., 1996), thus resulting in the difference between $z\delta_{+Glu}$ and $z\delta_{-Glu}$. To test this possibility, we measured the voltage dependence of T+2C modification by the permanently charged MTSET. The $\Delta z\delta$ value for MTSET (0.66 ± 0.04) as well as the absolute values of $z\delta_{+Glu}$ and $z\delta_{-Glu}$ (*shaded bars* in Fig. 3) were indistinguishable from those for MTSEA, indicating that any contribution of the uncharged form of MTSEA to measurements of the voltage dependence is negligible. Additionally, the reactivity of the neutral MTS reagent, MMTS, at T+2 was not voltage dependent in either the presence ($z\delta_{+Glu} = 0.02 \pm 0.04$) or absence ($z\delta_{-Glu} = 0.03 \pm 0.06$) of glutamate supporting the idea that our measurements of $z\delta$ reflect mainly changes in the transmembrane electrostatic potential rather than differences in pore properties (e.g., geometry or hydrophobicity) at various holding membrane potentials.

In summary, our results indicate that the electrostatic potential across the pore of the AMPAR channel as sensed by MTS reagents interacting with substituted cysteines undergoes significant changes during gating. In the presence of glutamate, $z\delta_{+Glu}$ changes monotonically from zero at the extracellular side to large positive values (~0.7) deeper in the pore. On the other hand, in the absence of glutamate, the voltage dependence is biphasic. The difference between $z\delta_{+Glu}$ and $z\delta_{-Glu}$ defines a bell-shaped function of the state-dependent difference in the electrostatic potential ($\Delta z\delta$) with an apparent maximum ($\Delta z\delta \sim 0.6$) in the middle of the extracellular vestibule.

Polyamine block does not account for the state-dependent difference in the electrostatic potential

The bell shape of $\Delta z\delta$ shown in Fig. 3 could potentially arise from a state-dependent occupation of the pore by polyamines, positively charged blockers of non-NMDAR channels (Bowie and Mayer, 1995; Donevan and Rogawski, 1995; Isa et al., 1995; Kamboj et al., 1995; Koh et al., 1995). We therefore examined the effect of polyamines on $\Delta z\delta$. To characterize polyamine block, we measured the voltage dependence of glutamate-activated currents using voltage ramps (Fig. 4 *A*). Current-voltage (*I-V*) curves were leak subtracted and corrected for the reversal potential yielding normalized conductance-voltage (*G-V*) plots (Fig. 4 *B*), which then were fitted with Eq. 5 over the range of −100–20 mV (see Methods). Parameters of polyamine block (Table 1) for wt′ were similar to those previously reported for wild-type GluR-6 channels (Panchenko et al., 1999, 2001). In GluR-6 channels, key determinants of polyamine block are a conserved aspartate (D586 in GluR-A) and the Q/R site (Q582 in GluR-A) in the M2 loop. Supporting this idea, the *G-V* curves for D586W/T+2C (Fig. 4 *B*) and D586C could not be well fitted by Eq. 5 (Table 1). Similarly, a glycine substitution at the Q/R site (Q582G) in Q582G/T+2C

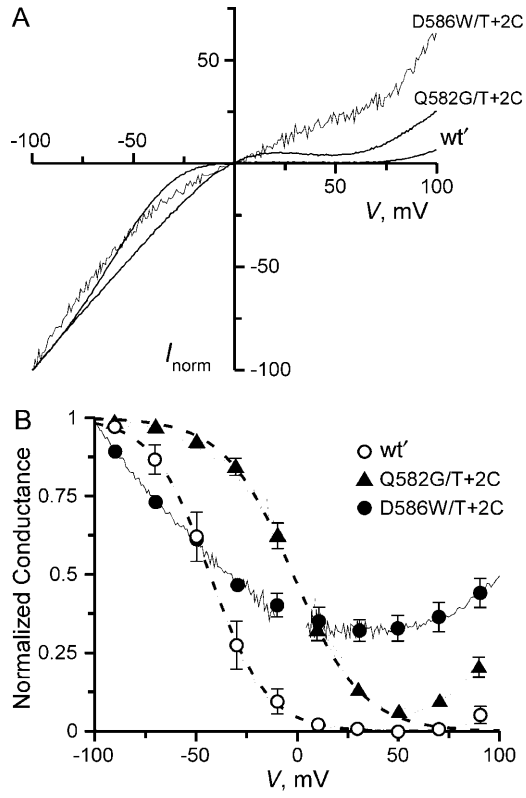

FIGURE 4 Changes in polyamine block caused by mutations in the M2 loop. (*A*) Example leak-subtracted current-voltage (*I-V*) curves for wt′, Q582G/T+2C, and D586W/T+2C channels. Current amplitudes were normalized to that at −100 mV. (*B*) Conductance, normalized to that at −100 mV, G_{norm}, as a function of the membrane voltage, *V*. Symbols show the mean G_{norm} values ($n = 7$–11) plotted at 20-mV intervals. Continuous curves are *G-V* plots derived from current records shown in panel *A* for wt′ and Q582G/T+2C and the averaged one for D586W/T+2C. Dashed lines show fits of Eq. 5 over the range of −100–20 mV for wt′ and Q582G/T+2C channels.

channels produced a 40-mV rightward shift in the *G-V* curve relative to wt′ (Fig. 4 *B*; Table 1). Compared to wt′, polyamine block in other mutant channels was either unchanged (L−5C and T+2C) or enhanced (L+5C and F+8C). The increased sensitivity to polyamines in L+5C and F+8C channels may be due to remote effects of cysteine substitutions on conformation of the binding site for polyamines in the intracellular vestibule. Alternatively, the introduced cysteines may form an additional binding site for polyamines in the extracellular vestibule.

Compared to wt′, polyamine block was significantly different in Q582G/T+2C and D586W/T+2C channels, whereas essentially the same in T+2C channels (Table 1). However, the $\Delta z\delta$ values measured for all three mutants (0.63 ± 0.02 for T+2C, 0.67 ± 0.02 for Q582G/T+2C, and 0.66 ± 0.02 for D586W/T+2C) were indistinguishable (Fig. 3). Hence, polyamine block makes no apparent contribution to the state-dependent difference in the membrane electric field sensed by MTS reagents at T+2C.

DISCUSSION

We used the voltage dependence of the rate of modification of substituted cysteines as a tool to probe the electrostatic potential across the pore of the GluR channel. The interpretation of our results is limited by the assumptions of the substituted cysteine accessibility method (Karlin and Akabas, 1998). For example, we assume that the cysteine (as well as other) substitutions do not alter greatly the structure of the protein. Additionally, we assume that the MTS reagents themselves do not change significantly the distribution of the electrostatic potential inside the pore. Although this assumption may not be completely correct for the absolute values of $z\delta$, it seems likely that the corresponding errors would be minimized or canceled out when comparing $z\delta$ values for different positions in the pore as well as considering the state-dependent differences ($\Delta z\delta$).

State-dependent differences in the electrostatic potential in the pore of the AMPAR channel

The distribution of the membrane electric potential across the pore of AMPAR channel is significantly different in the closed and open states (Figs. 3 and 5 *A*). This state-dependent difference in electric potential could arise from a number of factors including:

1. Changes in pore geometry. This phenomenon occurs, for example, in K^+ channels (Jiang et al., 2002), to which GluR channels are structurally related. In KcsA channels, where the intracellular gate at the crossing point of TM2 helices is closed, the membrane electric potential drops fairly uniformly across the entire length of the pore. In contrast, in MthK channels, where the intracellular gate is open, the potential drops solely across the selectivity filter formed by the P loop. This state-dependent difference arises because during gate opening the intracellular vestibule of K^+ channel becomes wide and equipotential with the cytoplasmic solution. Like in K^+ channels (although inverted in the membrane), the GluR extracellular vestibule widens with channel opening (Sobolevsky et al., 2002, 2003). In contrast to K^+ channels, however, the membrane electric potential is more concentrated in the closed rather than in the open state (Fig. 5 *A*).
2. A differential distribution of surface charges in the closed and open states. This alternative seems unlikely because surface charges in the extracellular vestibule make no apparent contribution to ion permeation in AMPAR channels (Jatzke et al., 2002). In addition, one would anticipate that surface charges would cause stronger state-dependent differences in the modification rate closer to the membrane surface. Instead, the strongest state-dependent

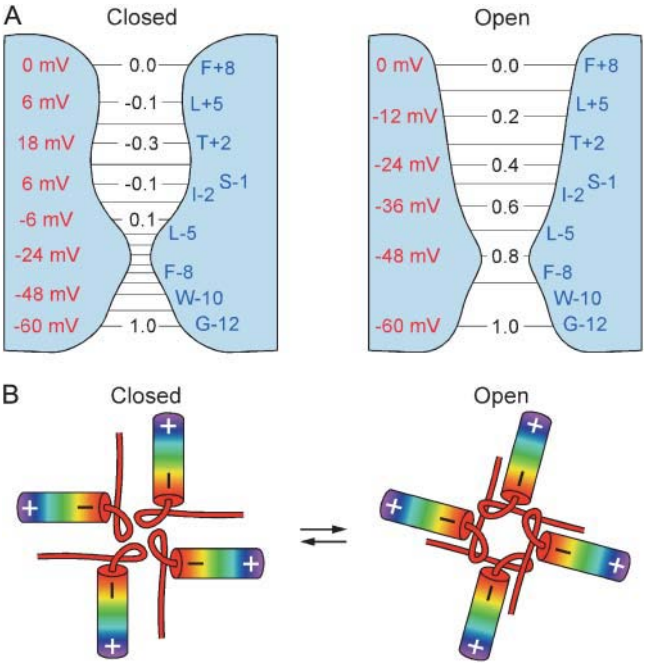

FIGURE 5 State-dependent distribution of the membrane electric field across the pore of AMPAR channel and the hypothesis of moving M2 loop dipoles. (*A*) Apparent distribution of the membrane electric field sensed by MTS reagents along the pore of AMPAR channel in the closed (*left*) and open (*right*) states. The $z\delta$ values estimated for MTSEA in the previous study (Sobolevsky et al., 2003) and in this study (Fig. 3) are shown in the center of the pore. The electric potential (in mV) sensed by MTS reagents at the corresponding vertical level at $V_h = -60$ mV is indicated to the left of the pore. Accessible positions in M3 used as reference points are indicated to the right of the pore. (*B*) The model of movement of the M2 loop dipoles during gating. Cylinders represent the polar α-helical regions of the M2 loops viewed from the extracellular side perpendicular to the plane of membrane. Blue and red indicate the N-terminal (positive) and C-terminal (negative) ends of the M2 α-helix dipoles. In the open state (*right*), the negative ends of the M2 loop dipoles are centered at the ion conduction pathway. In the closed state (*left*), the negative ends turn away from the center of the pore, changing the distribution of the membrane electric field inside the AMPAR channel.

difference was observed for positions located in the middle of the extracellular vestibule (T+2) with no apparent difference in the voltage dependence of modification rate for the most external position F+8 (Fig. 3).

3. A differential occupation of the pore in the closed and open states by positively charged polyamines. To test this hypothesis, we generated GluR-A mutant channels with greatly reduced sensitivity to polyamines in the open state. Substitutions were introduced at the Q/R site (Q582G substitution in Q582G/T+2C channels) or at the conserved negative aspartate in M2 (D586W substitution in D586W/T+2C channels). Similar to the homologous mutations in GluR-6 (Panchenko et al., 1999, 2001), Q582G and D586W strongly disrupted polyamine block (Fig. 4; Table 1). However, $\Delta z\delta$ values for Q582G/T+2C and D586W/T+2C channels were indistinguishable from those for T+2C channels (Fig. 3). Therefore, a differential occupation of the pore by polyamines is unlikely to explain state-dependent difference in the distribution of the membrane electric field in the pore of AMPAR channels.
4. Movement of electric charges or dipoles inside the channel pore during gating. The only charged residue in the pore region of the AMPAR channel (encompassing the M1, M2, M3, and M4 domains of GluR-A subunit) is the negatively charged aspartate (D586) located in the extended region of the M2 loop (Fig. 1 *B*). Although substitutions of this residue do indeed affect the membrane voltage sensed by MTS reagents (Fig. 3), they neither eliminate the state-dependent difference in $\Delta z\delta$ at this position (~0.29 for D586C), nor change it significantly at T+2 (~0.63 for T+2C and ~0.66 for D586W/T+2C).

Hence, the state-dependent changes in the membrane electric potential across the pore of the AMPAR channel are unlikely to be predominantly due to changing pore geometry, surface charges, polyamine block, or movement of charged residues during gating. Rather, based on a potential homology to inward-rectifier K^+ channels (see below), we propose that these state-dependent changes arise from reorientation of dipoles inside the channel, specifically those associated with the α-helix in the M2 loop.

Hypothesis of moving M2 dipoles and implications to GluR structure and gating

Major parts of the pore-lining segments M2 and M3 in the GluR channel are presumably α-helical (Kuner et al., 1996, 2001; Panchenko et al., 2001; Sobolevsky et al., 2003). Both M2 and M3 contain polar residues (Fig. 1 *A*), but because these residues are distributed equally on the surface of the α-helix, they are unlikely to create the strong electric field responsible for the observed state-dependent differences in $z\delta$ (Fig. 3). On the other hand, an α-helix itself has a dipole with its C-terminus having a partial negative charge. Indeed, the orientation of pore α-helices is critical to selectivity, permeation, and gating in K^+, Cl^-, and aquaporin channels (Doyle et al., 1998; Roux and MacKinnon, 1999; Murata et al., 2000; Dutzler et al., 2002, 2003; Kuo et al., 2003). In KcsA channel, for example, partial negative charges of the P-loop helices are oriented toward the water-filled cavity in the intracellular vestibule, changing the distribution of the electric field in a manner that facilitates permeation of positively charged K^+ ions through the pore. Given the structural homology between pore-lining domains in GluR (M2 loop and M3) and K^+ (P loop and TM2) channels (Kuner et al., 2003; Wollmuth and Sobolevsky, 2004), the negative poles of the M2 loop α-helices are presumably directed toward the center of the extracellular vestibule in GluR channel, at least in certain activation states (Kuner et al., 2001).

A movement of the M2 loops in GluR channels illustrated in Fig. 5 *B* would account for the results of this study. In the open state, the negative ends of the M2 α-helices are pointing toward the center of the pore facilitating the passage of permeant ions through it and contributing to the uniform membrane electric potential across the pore. In the closed state, the M2 dipoles are rotated away from the center of the pore changing the distribution of the membrane electric field in the middle of the extracellular vestibule (Fig. 5 *A*). Based on crystal structures, a similar gating-related movement of the P loops was proposed in inward-rectifier bacterial K^+ channels KirBac1.1 (Kuo et al., 2003). According to the moving dipoles hypothesis illustrated in Fig. 5 *B*, the M2 loops undergo significant displacement during GluR gating. Because these domains form the narrowest part of GluR channel pore (Kuner et al., 1996, 2001; Wollmuth et al., 1996), their gating-related movement is consistent with the idea of the activation gate associated with M2 (Beck et al., 1999; Sobolevsky et al., 2002).

Although the moving dipoles model illustrated in Fig. 5 *B* can account for the difference in the membrane electric potential sensed by MTS reagents in the closed and open states, many aspects of this model remain unclear. For example, what molecular and physical mechanisms define the negative values of $z\delta$ in the middle of the extracellular vestibule in the closed state (Fig. 3)? Which particular residues in the pore-lining domains form the gate for permeant ions? How are movements of M3 coupled to movements of the M2 loop? Finally, what are the structural features of the gating domains that allow multiple conductance levels in AMPAR channels (Rosenmund et al., 1998; Smith and Howe, 2000)? Additional experiments and approaches will be necessary to fully address these issues.

We thank Vyacheslav B. Yelshansky and Martin Prieto for comments on the manuscript.

This work was supported by National Institutes of Health RO1 grants from the National Institute of Neurological Disorders and Stroke (NS39102) and the National Institute of Mental Health (MH066892) (L.P.W.).

REFERENCES

Beck, C., L. P. Wollmuth, P. H. Seeburg, B. Sakmann, and T. Kuner. 1999. NMDAR channel segments forming the extracellular vestibule inferred from the accessibility of substituted cysteines. *Neuron.* 22:559–570.

Bowie, D., and M. L. Mayer. 1995. Inward rectification of both AMPA and kainate subtype glutamate receptors generated by polyamine-mediated ion channel block. *Neuron.* 15:453–462.

Dingledine, R., K. Borges, D. Bowie, and S. F. Traynelis. 1999. The glutamate receptor ion channels. *Pharmacol. Rev.* 51:7–61.

Doble, A. 1999. The role of excitotoxicity in neurodegenerative disease: implications for therapy. *Pharmacol. Ther.* 81:163–221.

Donevan, S. D., and M. A. Rogawski. 1995. Intracellular polyamines mediate inward rectification of Ca^{2+}-permeable alpha-amino-3-hydroxy-5-methyl-4-isoxazolepropionic acid receptors. *Proc. Natl. Acad. Sci. USA.* 92:9298–9302.

Doyle, D. A., J. Morais Cabral, R. A. Pfuetzner, A. Kuo, J. M. Gulbis, S. L. Cohen, B. T. Chait, and R. MacKinnon. 1998. The structure of the potassium channel: molecular basis of K^+ conduction and selectivity. *Science.* 280:69–77.

Dutzler, R., E. B. Campbell, M. Cadene, B. T. Chait, and R. MacKinnon. 2002. X-ray structure of a ClC chloride channel at 3.0 A reveals the molecular basis of anion selectivity. *Nature.* 415:287–294.

Dutzler, R., E. B. Campbell, and R. MacKinnon. 2003. Gating the selectivity filter in ClC chloride channels. *Science.* 300:108–112.

Hille, B. 2001. Ion Channels of Excitable Membranes, 3rd Ed. Sinauer Associates, Sunderland, MA.

Holmgren, M., Y. Liu, Y. Xu, and G. Yellen. 1996. On the use of thiol-modifying agents to determine channel topology. *Neuropharmacology.* 35:797–804.

Isa, T., M. Iino, S. Itazawa, and S. Ozawa. 1995. Spermine mediates inward rectification of Ca^{2+}-permeable AMPA receptor channels. *Neuroreport.* 6:2045–2048.

Jatzke, C., J. Watanabe, and L. P. Wollmuth. 2002. Voltage and concentration dependence of Ca^{2+} permeability in recombinant glutamate receptor subtypes. *J. Physiol.* 538:25–39.

Jiang, Y., A. Lee, J. Chen, M. Cadene, B. T. Chait, and R. MacKinnon. 2002. The open pore conformation of potassium channels. *Nature.* 417: 523–526.

Jones, K. S., H. M. VanDongen, and A. M. VanDongen. 2002. The NMDA receptor M3 segment is a conserved transduction element coupling ligand binding to channel opening. *J. Neurosci.* 22:2044–2053.

Kamboj, S. K., G. T. Swanson, and S. G. Cull-Candy. 1995. Intracellular spermine confers rectification on rat calcium-permeable AMPA and kainate receptors. *J. Physiol.* 486:297–303.

Karlin, A., and M. H. Akabas. 1998. Substituted-cysteine accessibility method. *Methods Enzymol.* 293:123–145.

Koh, D. S., N. Burnashev, and P. Jonas. 1995. Block of native Ca^{2+}-permeable AMPA receptors in rat brain by intracellular polyamines generates double rectification. *J. Physiol.* 486:305–312.

Kohda, K., Y. Wang, and M. Yuzaki. 2000. Mutation of a glutamate receptor motif reveals its role in gating and delta2 receptor channel properties. *Nat. Neurosci.* 3:315–322.

Kuner, T., C. Beck, B. Sakmann, and P. H. Seeburg. 2001. Channel-lining residues of the AMPA receptor M2 segment: structural environment of the Q/R site and identification of the selectivity filter. *J. Neurosci.* 21:4162–4172.

Kuner, T., P. H. Seeburg, and H. Robert Guy. 2003. A common architecture for K^+ channels and ionotropic glutamate receptors? *Trends Neurosci.* 26:27–32.

Kuner, T., L. P. Wollmuth, A. Karlin, P. H. Seeburg, and B. Sakmann. 1996. Structure of the NMDA receptor channel M2 segment inferred from the accessibility of substituted cysteines. *Neuron.* 17:343–352.

Kuo, A., J. M. Gulbis, J. F. Antcliff, T. Rahman, E. D. Lowe, J. Zimmer, J. Cuthbertson, F. M. Ashcroft, T. Ezaki, and D. A. Doyle. 2003. Crystal structure of the potassium channel KirBac1.1 in the closed state. *Science.* 300:1922–1926.

Murata, K., K. Mitsuoka, T. Hirai, T. Walz, P. Agre, J. B. Heymann, A. Engel, and Y. Fujiyoshi. 2000. Structural determinants of water permeation through aquaporin-1. *Nature.* 407:599–605.

Panchenko, V. A., C. R. Glasser, and M. L. Mayer. 2001. Structural similarities between glutamate receptor channels and K^+ channels examined by scanning mutagenesis. *J. Gen. Physiol.* 117:345–360.

Panchenko, V. A., C. R. Glasser, K. M. Partin, and M. L. Mayer. 1999. Amino acid substitutions in the pore of rat glutamate receptors at sites influencing block by polyamines. *J. Physiol.* 520:337–357.

Pascual, J. M., and A. Karlin. 1998. State-dependent accessibility and electrostatic potential in the channel of the acetylcholine receptor. Inferences from rates of reaction of thiosulfonates with substituted cysteines in the M2 segment of the alpha subunit. *J. Gen. Physiol.* 111:717–739.

Rosenmund, C., Y. Stern-Bach, and C. F. Stevens. 1998. The tetrameric structure of a glutamate receptor channel. *Science.* 280:1596–1599.

Roux, B., and R. MacKinnon. 1999. The cavity and pore helices in the KcsA K^+ channel: electrostatic stabilization of monovalent cations. *Science.* 285:100–102.

Smith, T. C., and J. R. Howe. 2000. Concentration-dependent substate behavior of native AMPA receptors. *Nat. Neurosci.* 3:992–997.

Sobolevsky, A. I., C. Beck, and L. P. Wollmuth. 2002. Molecular rearrangements of the extracellular vestibule in NMDAR channels during gating. *Neuron.* 33:75–85.

Sobolevsky, A. I., M. V. Yelshansky, and L. P. Wollmuth. 2003. Different gating mechanisms in glutamate receptor and K^+ channels. *J. Neurosci.* 23:7559–7568.

Stern-Bach, Y., S. Russo, M. Neuman, and C. Rosenmund. 1998. A point mutation in the glutamate binding site blocks desensitization of AMPA receptors. *Neuron.* 21:907–918.

Wilson, G. G., J. M. Pascual, N. Brooijmans, D. Murray, and A. Karlin. 2000. The intrinsic electrostatic potential and the intermediate ring of charge in the acetylcholine receptor channel. *J. Gen. Physiol.* 115:93–106.

Wollmuth, L. P., T. Kuner, P. H. Seeburg, and B. Sakmann. 1996. Differential contribution of the NR1- and NR2A-subunits to the selectivity filter of recombinant NMDA receptor channels. *J. Physiol.* 491:779–797.

Wollmuth, L. P., and A. I. Sobolevsky. 2004. Structure and gating of the glutamate receptor ion channel. *Trends Neurosci.* 27:321–328.